ACS OMEGA

Open Access

http://pubs.acs.org/journal/acsodf

Article

Green Synthesis of a Novel Cationic Surfactant Based on an Azo Schiff Compound for Use as a Carbon Steel Anticorrosion Agent

Kaseb D. Alanazi, Basmah H. Alshammari, Tahani Y. A. Alanazi, Odah A. Alshammari, Ashraf M. Ashmawy,* Meshari M. Aljohani, Reda Abdel Hameed, and Mohamed A. Deyab*

Cite This: *ACS Omega* 2023, 8, 49009−49016

Read Online

ACCESS | Metrics & More | Article Recommendations

ABSTRACT: The new cationic surfactant-based azo Schiff compound (azoS8) was prepared, characterized, and investigated as a corrosion inhibitor for carbon steel in 1 M HCl by means of electrochemical approaches in this study. The chemical structure of azoS8 has been verified by the FTIR and ^{1}H NMR spectra. According to the electrochemical system, the examined surfactant is a mixed-type inhibitor. The surfactant azoS8 was an adequate corrosion inhibitor, as evidenced by the reduction in corrosion current densities and the rise in coverage of the surface identified with an evolving inhibitor amount. When the surfactant azoS8 had been added, the capacitive cycle loops on the Nyquist plots were broader, and the dimension of these loops expanded with surfactant azoS8 concentration. This implies that the amount of surfactant azoS8 led to an improvement in the impedance of the steel electrode. The surfactant azoS8 adsorption system is well suited to the Langmuir adsorption isotherm. It was discovered that azoS8 had a Gibbs free energy change value of −27.72 kJ mol^{-1}, which is a mixed adsorption mechanism containing both physisorption and chemisorption.

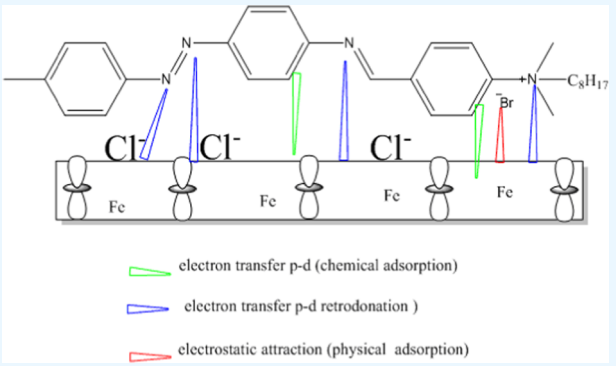

1. INTRODUCTION

Corrosion has always presented a significant challenge to the metal industry and its affiliated sectors. The detrimental impact of corrosion results in reduced durability, lower quality, and a shorter lifespan for metal products, consequently driving up industry costs due to the need for part replacements, damage to capital structures, or other necessary mitigation measures.[1−3] Metals can be negatively affected by corrosion, which can lead to their dissolution, causing them to lose their original shape and the beneficial properties they once possessed.[4−6] Many researchers aim to delay or prevent corrosion, with organic inhibitors being a preferred method due to their cost-effectiveness and high efficiency, typically added in very low concentrations to control corrosion in various industries, especially during processes like acid treatment of mild steel used in industries like petroleum, construction, and pipelines to prevent damage to the metal.[7−13]

Using organic molecules that have electronegative atoms (like N, S, P, and O), unsaturated bonds, and aromatic rings as a way to prevent corrosion is a cost-effective technique.[14−16] Schiff bases or azomethines considered a class of organic inhibitors used for this purpose, and they contain nitrogen atoms bonded to carbon atoms by double bonds which makes them easy to absorb because of lone pairs of electrons and high electron density.[1717] Due to the presence of, most azo derivatives are used as synthetic dyes. However, these compounds have also been recognized for their potential use in a variety of applications in different fields, as lubricating additives, heat transfer fluids, cosmetics, and corrosion inhibitors.[18−21] The flexibility in selecting additional components for the structure of azo dyes combined with the presence of nitrogen atoms in the azo linkage enables the design of molecules that meet the structural criteria of organic corrosion inhibitors. As a result, these molecules can be easily and strongly adsorbed onto the surface of steel.[21] Alkyl chains have an important role along with heteroatoms in metal protection against corrosion.[22] The hydrophobic properties of alkyl chains in organic inhibitors help in preventing contact between water molecules and the metal surface, and this leads to more area being covered on the metal surface, increasing the inhibition efficiency for organic molecules.[23,24] Various methods were employed by different authors to investigate the ability of azo dyes to inhibit corrosion.[25−28] They created three new azo

Received: September 5, 2023
Revised: November 17, 2023
Accepted: November 24, 2023
Published: December 14, 2023

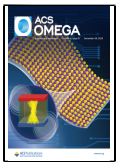

Scheme 1. Preparation Steps of azoS8

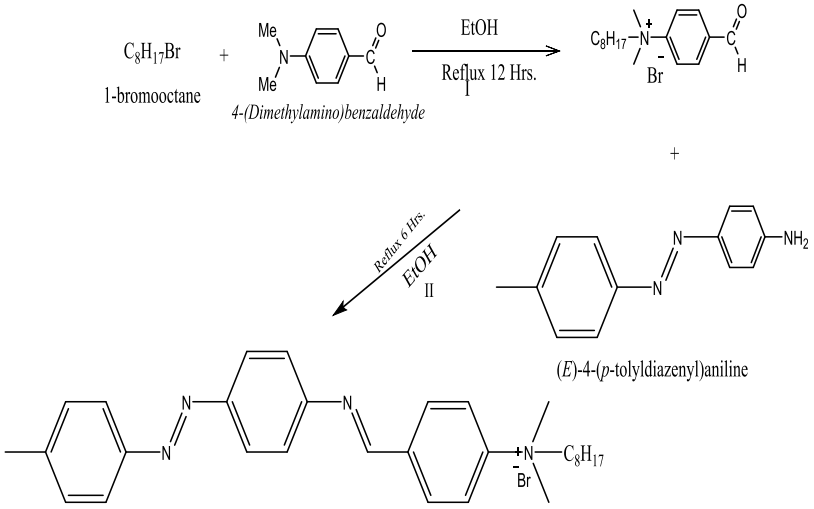

acetyl coumarin derivatives, Acetyl A, B, and Start B, and investigated their potential as mild steel corrosion inhibitors in 1 M HCl in their studies. The synthesized compounds were analyzed using FTIR and ^{1}H NMR. The researchers used impedance and polarization methods to test the compounds' anticorrosive potential. The results of the polarization tests showed that the presence of Acetyl A, B and Start B resulted in a significant decrease in corrosion current density compared to their absence, indicating that these compounds bind to active sites and inhibit corrosion. The inhibitory effectiveness of the compounds was Acetyl B (93.01%) > Acetyl A (92.23%) > Start B (85.29%) at the best concentration of 7.50×10^{-4} M.[28] The researchers observed that the Langmuir adsorption isotherm was followed when the inhibiting molecules were adsorbed on the surface of the mild steel. As a corrosion inhibitor for carbon steel (CS) in acidic solution, we created a novel molecule (azoS8) that contains an azo group, azo methane, and a chain length in the current study.

2. EXPERIMENTAL DETAILS

2.1. Materials. The experiments utilized CS with the following chemical composition (by weight): 0.093% carbon, 0.014% phosphorus, 0.011% silicon, 0.853% manganese, 0.025% chromium, 0.012% copper, 0.032% aluminum, 0.013% nickel, and the remaining consisting of iron. To prepare the corrosive media, we made a 1 M HCl solution by diluting 37% HCl (AR grade) with distilled water. The inhibitor dose was varied from 100 to 500 ppm.

2.2. Synthesis of Surfactant azoS8. The synthesis process for the surfactant involved two steps. First, the azo compound (azoS8) involves a two-step process: first, *p*-toluidine is diazotized with a nitrous acid source to form a diazonium salt. In the second step, this diazonium salt is coupled with an aniline compound under suitable conditions to yield the desired (*E*)-4-(*p*-tolyldiazenyl)aniline; this method is described in the literature.[29] In the second step, the surfactant *N*,*N*-dimethyl-*N*-octyl-4-((*E*)-((4-((*E*)-*p*-tolyldiazenyl)phenyl)imino)methyl)benzenaminium bromide was synthesized by heating 1-bromooctane with an equal amount of 4-(dimethylamino)benzaldehyde in absolute ethanol, in a 1:1 molar ratio. The reactants were refluxed for 12 h. Following that, the reaction mixture was cooled to ambient temperature. In the final step of the synthesis process, Schiff base compounds (azo) were produced by condensing *N*-decyl-4-formyl-*N*,*N*-dimethylbenzenaminium bromide with (*E*)-4-((4-methoxyphenyl)diazenyl)aniline in ethanol with a 1:1 molar ratio. The resulting compounds were recrystallized from ethanol. Scheme 1 depicts the compound structure of the synthesized (azoS8). The structure of the synthesized (azoS8) was confirmed using various analytical tools such as FTIR and ^{1}H NMR.

2.3. Methods. The electrochemical cell with three electrodes was employed to take measurements.[30] The working electrode used was CS and had a surface area of 1 cm^2, while a saturated calomel electrode (SCE) was utilized as the reference electrode. Additionally, a counter electrode made of a platinum wire was employed. The study conducted measurements using two electrochemical techniques, namely, electrochemical impedance spectroscopy (EIS) and potentiodynamic polarization (PP). Following the immersion of the electrode in the test solution for an hour, electrochemical impedance spectroscopy (EIS) was carried out at open-circuit voltage (OCV). A small alternating voltage perturbation of 10 mV was applied to the cell over a frequency range of 100 kHz to 20 mHz at a temperature of 298 K. Subsequently, PP was performed for anodic and cathodic polarization, with a scan rate of 5 mV s^{-1}. The aforementioned techniques were all carried out with a Gamry 3000 potentiostat/galvanostat/ZRA, and the data obtained were analyzed using Echem Analyst 7.[15,31] Three repetitions were performed for each test to ensure significant repeatability of the results.

A JEOL-JSM-6510 scanning electron microscope (SEM) was utilized to characterize the surface.

3. RESULTS AND DISCUSSION

3.1. Characterization of the Prepared Inhibitor azoS8. The FTIR and ^{1}H NMR spectra of the inhibitor are presented in Figures 1 and 2, respectively. The spectra were analyzed to determine the active groups and specifications of the inhibitor. In the case of azoS8, the bands observed at 3460 cm^{-1} were assigned to the stretching vibrations of the hydrogen-bonded H_2O molecules (CH−H_2O).[32] C−H stretching vibrations were observed around 2920 cm^{-1} due to the aliphatic chain in addition to Ar−H stretching vibrations around 3020 cm^{-1}. The peaks at 1634 and 1490 cm^{-1} are assigned to the stretching vibration of C═N and N═N, respectively.[18] The FTIR

https://doi.org/10.1021/acsomega.3c06710
ACS Omega 2023, 8, 49009−49016

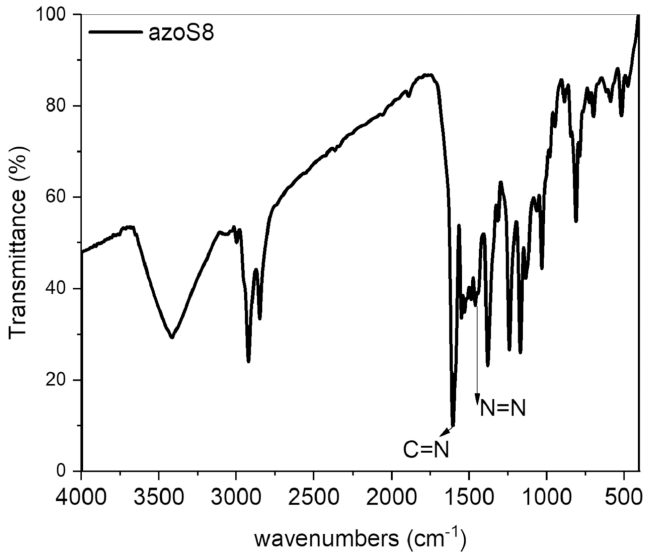

Figure 1. FTIR spectra of azoS8.

analysis revealed the presence of infrared (IR) bands that can be attributed to the chemical structures of newly synthesized azoS8. Another technique used to characterize azoS8 is the proton nuclear magnetic resonance (^{1}H NMR) spectrum. The signals between 0.8 and 1.6 ppm correspond to the protons in the aliphatic chain of the decyl group. The signal at around 2.8−3.0 ppm corresponds to the protons in the *N*,*N*-dimethylbenzenaminium group.The signal at around 3.6−3.8 ppm corresponds to the protons in the methoxy group.The signals in the range of 6.6−7.7 ppm correspond to the protons in the aromatic rings of the molecule.The signal at 9.6 ppm corresponds to the proton in the N═CH group. This peak is typically a sharp singlet due to the lack of proton coupling to neighboring protons. Overall, the ^{1}H NMR spectrum can provide valuable information about the identity and structure of azoS8.

3.2. Electrochemical Evaluation. *3.2.1. Open-Circuit Potential (OCP).* Figure 3 depicts a graph of the open-circuit potential as a function of time for CS in a 1 M HCl solution, with and without varying amounts of azoS8 at a temperature of 298 K. After 200 s, the OCP reached a steady-state value that remained constant and did not change over time.

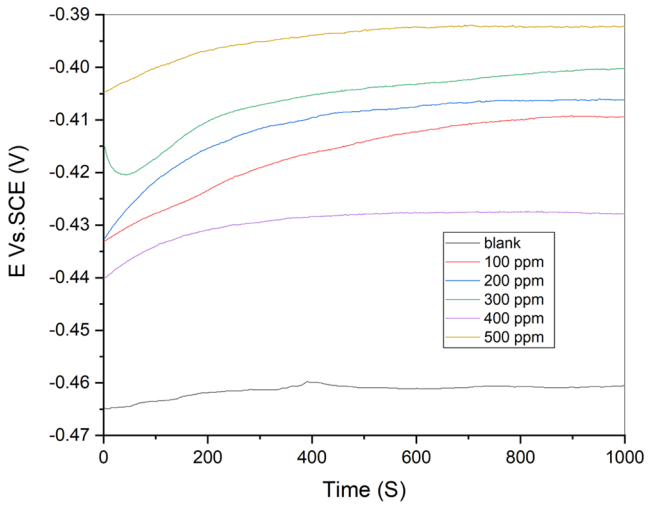

Figure 3. Open-circuit potential (OCP) as a function of time for carbon steel in a 1 M HCl solution, with and without varying amounts of azoS8 at a temperature of 298 K.

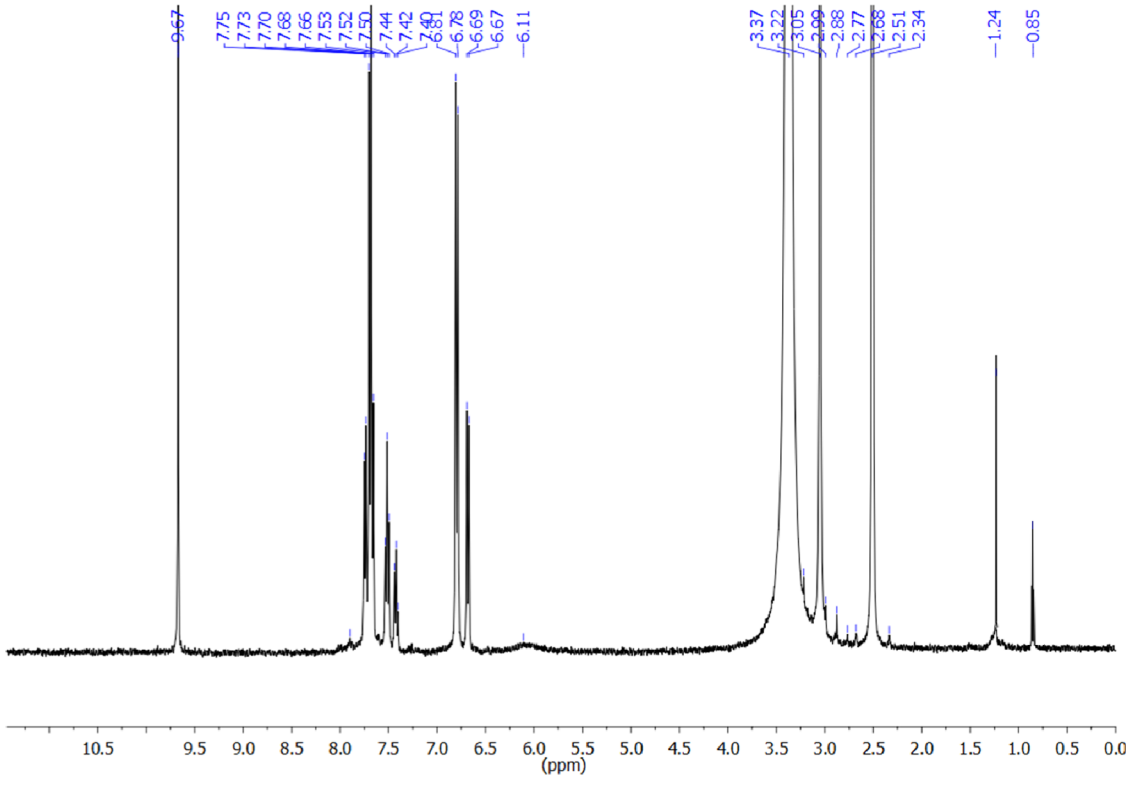

Figure 2. ^{1}H NMR spectra of azoS8.

https://doi.org/10.1021/acsomega.3c06710
ACS Omega 2023, 8, 49009−49016

3.2.2. Potentiodynamic Polarization Measurements. PP study was carried out to explore anticorrosion properties of the newly created inhibitor azoS8. During this study, CS was utilized as the working electrode. Figure 4 shows the

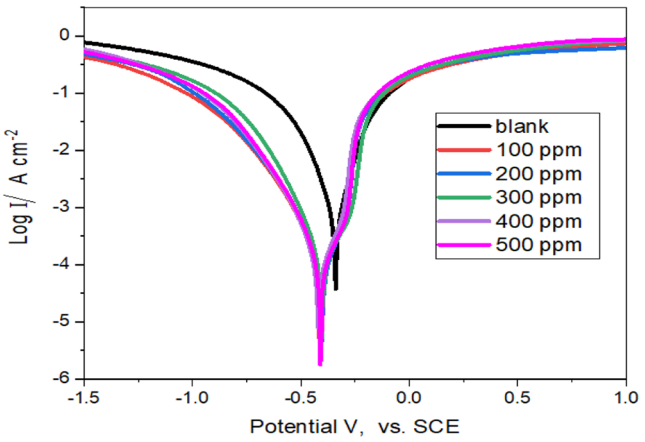

Figure 4. Polarization curves for carbon steel in a 1 M HCl solution, with and without varying amounts of azoS8 at a temperature of 298 K.

polarization curves of CS in a 1 M HCl solution at 298 K, both with and without various concentrations of azoS8 (ranging from 100 to 500 ppm). Table 1 presents the electrochemical parameters, including corrosion current density (I_{corr}), corrosion potential (E_{corr}), anodic Tafel slope (β_a), and cathodic Tafel slope (β_c), as well as inhibition efficiency (η_{pot}%), that were obtained from the experiment. The study revealed that there was a change in the value of β_c as the concentration of the inhibitor increased. The effect of the inhibitor on hydrogen evolution kinetics was analyzed, and an alteration in the anodic Tafel slope β_a was noted, which was possibly due to the adsorption of chloride ions or inhibitor molecules onto the surface of the metal. With the increase in the inhibitor concentration, the corrosion current density (I_{corr}) decreased due to the increased adsorption of the inhibitor. Additionally, azoS8 was found to cause a slight shift in the corrosion potential (E_{corr}). The inhibited systems displayed E_{corr} values that were lower than 80 mV in comparison to the acid blank, indicating that the surfactants examined in the study are of a mixed-type inhibitor.[33] The inhibition efficiency (η_{pot}%) and surface coverage (θ) were calculated using the following formulas[30]

$$\theta = \frac{I^0_{corr} - I_{corr}}{I^0_{corr}} \quad (1)$$

$$\eta_{Pot}\% = \theta \times 100 \quad (2)$$

where I_{corr} and $I_{corr}{}^0$ denote the inhibited and uninhibited corrosion current densities, respectively.

The findings showed that as the concentration of the inhibitor increased, there was a reduction in the corrosion current densities and an increase in the surface coverage (θ). These results indicated that azoS8 was an efficient corrosion inhibitor that could effectively prevent the dissolution of steel in a solution of 1 M hydrochloric acid. This beneficial effect was attributed to the formation of anodic protective films on the electrode surface, which served as a protective barrier against the corrosive impact of the acid.[25,34] At 500 ppm of azoS8, the greatest inhibition efficiency (i.e., 91.25%) was attained. Above this concentration, there was a little change in the inhibition effectiveness.

3.2.3. Electrochemical Impedance Spectroscopy (EIS). The aim of the EIS is to examine how quickly the steel corrodes in a 1 M HCl corrosive solution in different doses of synthesized inhibitor. Figure 5 shows the Nyquist and Bode plots obtained when inhibitor was present and when -it was absent. Although the shape of the plots remained the same at different concentrations, the height or intensity varied for each concentration. A higher concentration resulted in a higher peak, indicating greater resistance to the solution. One possible explanation for this observation is that the artificially created inhibitor may has created a shieldlike barrier on the surface of the steel, resulting in a decrease in the rate of corrosion when exposed to the corrosive environment. Furthermore, the Nyquist plots displayed larger capacitive loops when the inhibitor was present, and the size of these loops increased with increasing inhibitor concentration. This suggests that the impedance of the steel electrode that was inhibited also increased because of the inhibitor concentration.[34,35]

The capacitance loops demonstrate that the corrosion of CS and the formation of a surface barrier are mainly governed by the electron transfer mechanism.[36] To examine the impedance of CS in the presence of inhibitor in 1 M HCl, the experimental data were fitted using the equivalent circuit model illustrated in Figure 5. This model includes three components: R_s (R_u) to represent the solution resistance, R_{ct} (R_p) to represent the charge transfer resistance, and (C_{dl}) to represent the double-layer capacitance on the metal surface.[33] Table 2 represents that the introduction of an additive to a 1 M HCl solution leads to an increase in the R_{ct} values, signifying that the charge transfer pathways are impeded. The inhibition efficiency ($IE_{(EIS)}$%) and θ were computed using eqs 3 and 4[37]

$$IE_{EIS}\% = \theta \times 100 = \frac{R_{ct(inh)} - R_{ct(unh)}}{R_{ct(inh)}} \times 100 \quad (3)$$

where $R_{ct(inh)}$ and $R_{ct(unh)}$ denote the charge transfer resistances in the presence and absence of an inhibitor, respectively.

Table 1. Potentiodynamic Electrochemical Parameters for CS Immersed in 1.0 M HCl, in Absence and Presence of Different Concentrations of azoS8 at 298 K

C (ppm)	β_a (mV dec^{-1})	β_c (mV dec^{-1})	I_{corr} (uA cm^{-2})	$-E_{corr}$ vs SCE (mV)	θ	η_{pot}%
blank	412.4	414.2	918	396		
100	174.6	151.0	139	413	0.8485	84.85
200	173.2	153.9	137	403	0.8507	85.07
300	173.5	119.7	133	404	0.8551	85.51
400	139.0	129.4	115	418	0.8747	87.47
500	125.6	122.2	80	409	0.9125	91.25

https://doi.org/10.1021/acsomega.3c06710
ACS Omega 2023, 8, 49009−49016

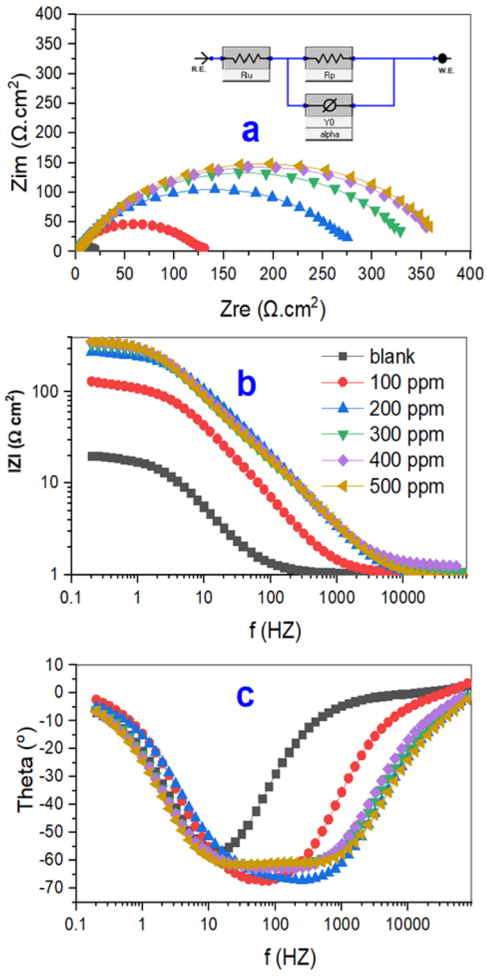

Figure 5. (a) Nyquist, (b) Bode, (c) Bode−phase angle plots and equivalent circuit model (inset in a) for carbon steel in a 1 M HCl solution, with and without varying amounts of azoS8 at a temperature of 298 K.

$$C_{dl} = (y_0 R_{ct}^{1-n})^{1/n} \quad (4)$$

In the equation, the CPE exponent is represented by n, and Y_0 is the CPE constant. The value of n, which falls between 0 and 1, indicates the deviation from ideal behavior. According to Table 2, the use of the inhibitor led to a reduction in the C_{dl} value, indicating that either the local dielectric constant decreased or the thickness of the electrical double layer increased. This suggests that the azoS8 molecules function by forming a protective layer on the metal surface.[38]

3.3. Adsorption Studies. Adsorption isotherms are frequently employed to comprehend the interaction between inhibitor molecules and active metal surface sites. Electrochemical experiments are conducted to determine the surface coverage (θ) at varying inhibitor concentrations (C_{azoS8}), and different isotherms are utilized to determine the most suitable fit that characterizes the behavior of the inhibitor molecules. The Langmuir isotherm has been found to be the most effective in describing the adsorption process. This isotherm and the Gibbs free energy change (ΔG_{ads}^0) are represented by the following relations

$$\frac{C_{inh}}{\theta} = \frac{1}{K_{ads}} + C_{inh} \quad (5)$$

$$\Delta G_{ads}^0 = -RT \ln (55.5\, K_{ads}) \quad (6)$$

In the relations, the universal gas constant is represented by R (with a value of 8.314 J mol^{-1} K^{-1}), 55.5 denote the molar concentration of pure water, and T represents the thermodynamic temperature in Kelvin. The adsorption constant is denoted by K_{ads}. C_{inh} is the concentration of the azoS8, and θ is the surface coverage.[26,39] Figure 6 shows the Langmuir adsorption isotherm for the adsorption of azoS8 on the carbon steel surface. The value of ΔG_{ads}^0 for azoS8 was found to be −27.72 kJ mol^{-1}. The negative value of ΔG_{ads}^0 indicates that the azoS8 molecules have a strong tendency to be adsorbed onto the steel surface and that the layer formed is stable. ΔG_{ads}^0 values below −20 kJ mol^{-1} are typically linked to physical adsorption, which occurs through electrostatic attraction between the charged molecules and the charged metal. On the other hand, ΔG_{ads}^0 values greater than −40 kJ mol^{-1} are associated with chemisorption, in which charge

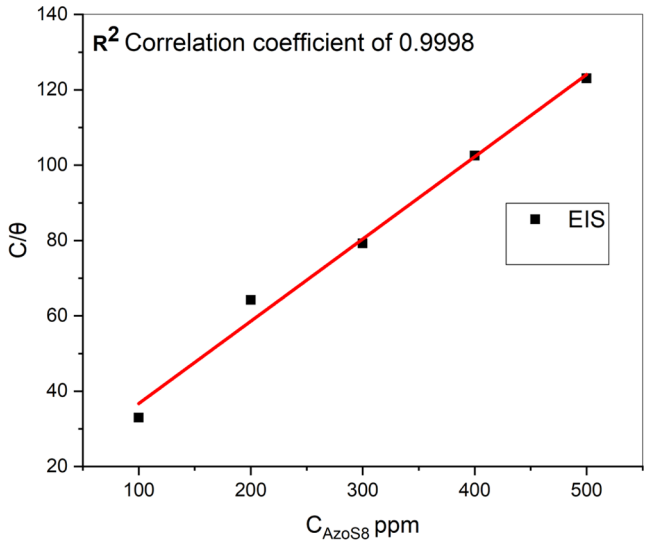

Figure 6. Langmuir adsorption isotherm of azoS8 at 298 K.

Table 2. EIS Parameters for CS Immersed in 1.0 M HCl in the Absence and Presence of Different Concentrations of azoS8 at 298 K

C (ppm)	R_{ct} (Ω·cm²)	R_s (Ω·cm²)	Y_0 (Ω^{-1} s^n cm^{-2})	C_{dl} (F cm^{-2})	X²	θ	$IE_{(EIS)}$ %
blank	18.87	1.038	4.48×10^{-3}	0.339×10^{-3}	3.53×10^{-4}		
100	120.2	1.031	5.37×10^{-4}	3.60×10^{-4}	1.33×10^{-3}	0.8430	84.30
200	277.0	0.870	2.54×10^{-4}	1.41×10^{-4}	8.9×10^{-4}	0.9319	93.19
300	361.2	1.022	3.85×10^{-4}	2.18×10^{-4}	2.32×10^{-3}	0.9478	94.78
400	385.6	1.195	3.45×10^{-4}	1.99×10^{-4}	1.54×10^{-3}	0.9511	95.11
500	406.8	0.8475	3.98×10^{-4}	2.81×10^{-4}	2.94×10^{-3}	0.9536	95.36

https://doi.org/10.1021/acsomega.3c06710
ACS Omega 2023, 8, 49009−49016

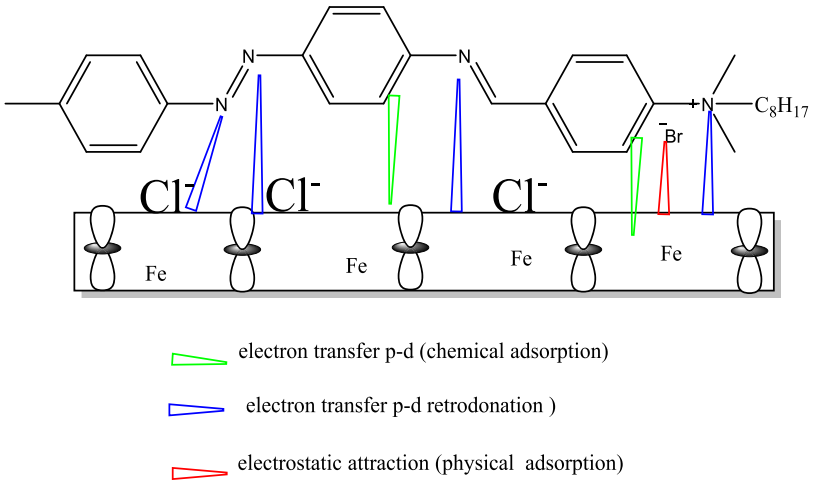

Figure 7. Adsorption of azoS8 on the carbon steel surface.

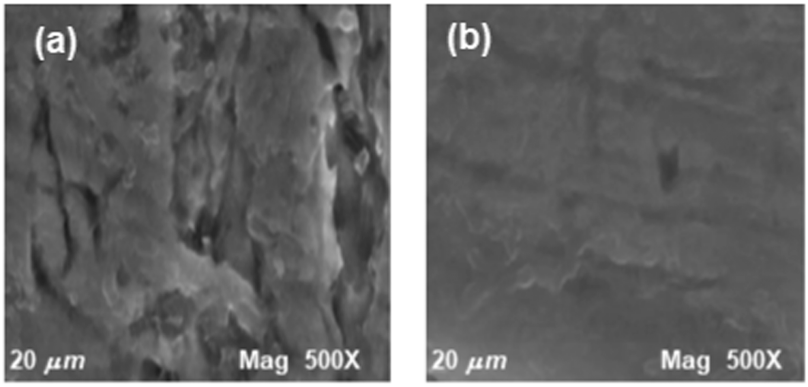

Figure 8. SEM photos of the surface of carbon steel in 1.0 M HCl, both in the absence (a) and presence (b) of 500 ppm azoS8.

sharing or transfer from organic molecules to the metal surface leads to the formation of a coordinate bond.[40] The absolute values of ΔG_{ads}^{0}, falling within the range of −20 into −40 kJ mol^{-1}, suggest that the adsorption of azoS8 onto the steel surface involves a mixed adsorption mechanism comprising both physisorption and chemisorption. The presence of three aromatic moieties in azoS8 is a crucial factor in the adsorption and protection processes. The unshared electron pairs of π-bonds in these moieties act as potential reaction centers (donation reaction centers) for the vacant d-orbital of the iron metal via a chemisorption mechanism. Moreover, the presence of the ammonium cation (N^+) and Br^- anions in azoS8 results in electrostatic attraction between them and the charged steel surface via the physisorption mechanism. The availability of multiple active sites for adsorption through physical electrostatic attraction and chemisorption, as demonstrated in Figure 7, enhances the surfactants' ability to protect the steel surface.[39]

Surface characterization (SEM analysis) of carbon steel surfaces in 1.0 M HCl, both in the absence and presence of 500 ppm of azoS8, provided confirmation of adsorption of azoS8 (Figure 8a). The metal surface of carbon steel experienced significant cracks and corrosion after immersion in a 1.0 M HCl solution (Figure 8a). Additionally, the image in Figure 8b showed a smooth carbon steel surface with 500 ppm of azoS8, demonstrating the remarkable degree of protection against corrosion obtainable through 500 ppm azoS8.

4. CONCLUSIONS

In the current study, the new cationic surfactant (azoS8) acted as a corrosion inhibitor for steel in 1.0 M HCl. The characterizations of azoS8 were confirmed by FTIR and ^{1}H NMR spectroscopies. The polarization results confirmed that azoS8 can be classified as a mixed-type inhibitor. The azoS8 adsorption system is well suited to the Langmuir adsorption isotherm. The new corrosion inhibitor azoS8 had a Gibbs free energy change value of −27.72 kJ mol^{-1}. EIS parameters suggested that azoS8 acted in a mixed adsorption mechanism comprising both physisorption and chemisorption.

AUTHOR INFORMATION

Corresponding Authors

Mohamed A. Deyab − *Egyptian Petroleum Research Institute (EPRI), Nasr City 11251 Cairo, Egypt;* orcid.org/0000-0002-4053-4942; Email: madeyab@epri.sci.eg

Ashraf M. Ashmawy − *Chemistry Department, Faculty of Science (boys), Al-Azhar University, 11884 Nasr City, Egypt;* Email: ashraf_ashmawy2002@yahoo.com

Authors

Kaseb D. Alanazi − *Department of Chemistry, College of Science, University of Ha'il, 81442 Hail, Saudi Arabia*

Basmah H. Alshammari − *Department of Chemistry, College of Science, University of Ha'il, 81442 Hail, Saudi Arabia*

Tahani Y. A. Alanazi − *Department of Chemistry, College of Science, University of Ha'il, 81442 Hail, Saudi Arabia*

https://doi.org/10.1021/acsomega.3c06710
ACS Omega 2023, 8, 49009−49016

Odah A. Alshammari − *Department of Chemistry, College of Science, University of Ha'il, 81442 Hail, Saudi Arabia*
Meshari M. Aljohani − *Department of Chemistry, College of Science, Tabuk University, 71491 Tabuk, Saudi Arabia*
Reda Abdel Hameed − *Chemistry Department, Faculty of Science (boys), Al-Azhar University, 11884 Nasr City, Egypt; Basic Science Department, Preparatory Year, University of Ha'il, 1560 Hail, KSA;* orcid.org/0000-0003-2785-894X

Complete contact information is available at: https://pubs.acs.org/10.1021/acsomega.3c06710

Notes

The authors declare no competing financial interest.

■ ACKNOWLEDGMENTS

This research has been funded by Scientific Research Deanship at University of Ha'il, Saudi Arabia through project number **RG-23064.** The authors highly appreciate and introduce deep thanks for Scientific Research Deanship University of Ha'il, Saudi Arabia.

■ REFERENCES

(1) Javaherdashti, R. How corrosion affects industry and life. *Anti-Corros. Methods Mater.* **2000**, *47*, 30−34.
(2) Bender, R.; Féron, D.; Mills, D.; Ritter, S.; Bäßler, R.; Bettge, D.; De Graeve, I.; Dugstad, A.; Grassini, S.; Hack, T.; et al. Corrosion challenges towards a sustainable society. *Mater. Corros.* **2022**, *73* (11), 1730−1751.
(3) Lai, G. Y. *High-Temperature Corrosion and Materials Applications*; ASM international, 2007.
(4) Moncmanová, A. *Environmental Deterioration of Materials*; Wit Press, 2007; Vol. *21*.
(5) Singh, A. K.; Chugh, B.; Singh, M.; Thakur, S.; Pani, B.; Guo, L.; Kaya, S.; Serdaroglu, G. Hydroxy phenyl hydrazides and their role as corrosion impeding agent: A detail experimental and theoretical study. *J. Mol. Liq.* **2021**, *330*, No. 115605.
(6) Haque, J.; Srivastava, V.; Chauhan, D. S.; Lgaz, H.; Quraishi, M. A. Microwave-induced synthesis of chitosan Schiff bases and their application as novel and green corrosion inhibitors: experimental and theoretical approach. *ACS Omega* **2018**, *3* (5), 5654−5668.
(7) Ahmed ES, J.; Ganesh, G. M. A Comprehensive Overview on Corrosion in RCC and Its Prevention Using Various Green Corrosion Inhibitors. *Buildings* **2022**, *12* (10), 1682.
(8) Rani, B. E. A.; Basu, B. B. J. Green inhibitors for corrosion protection of metals and alloys: an overview. *Int. J. Corros.* **2012**, *2012*, No. 380217.
(9) Singh, A. K.; Singh, M.; Thakur, S.; Pani, B.; Kaya, S.; Ibrahimi, B. E.; Marzouki, R. Adsorption study of N (-benzo [d] thiazol-2-yl)-1-(thiophene-2-yl) methanimine at mild steel/aqueous H2SO4 interface. *Surf. Interfaces* **2022**, *33*, No. 102169.
(10) Brycki, B. E.; Kowalczyk, I. H.; Szulc, A.; Kaczerewska, O.; Pakiet, M. Organic corrosion inhibitors. *Corrosion inhibitors, principles and recent applications* **2018**, *3*, 33.
(11) Finšgar, M.; Jackson, J. Application of corrosion inhibitors for steels in acidic media for the oil and gas industry: A review. *Corros. Sci.* **2014**, *86*, 17−41.
(12) Rugmini Ammal, P.; Prajila, M.; Joseph, A. Effective inhibition of mild steel corrosion in hydrochloric acid using EBIMOT, a 1, 3, 4-oxadiazole derivative bearing a 2-ethylbenzimidazole moiety: Electro analytical, computational and kinetic studies. *Egypt. J. Pet.* **2018**, *27* (4), 823−833.
(13) Dharmaraj, E.; Pragathiswaran, C.; Govindhan, P.; Arockia Sahayaraj, P.; John Amalraj, A.; Dharmalingam, V. Corrosion inhibition of mild steel by natural product compound. *Int. J. Res. Pharm. Chem.* **2017**, *7* (1), 132.
(14) Ashmawy, A. M.; El-Sawy, A. M.; Khalil, H. F. Synthesis of novel liquid crystal compound and study of its behavior as corrosion inhibitor for mild steel in acidic medium (1 M) HCl. *Mol. Cryst. Liq. Cryst.* **2022**, *736* (1), 9−29.
(15) Nessim, M. I.; Zaky, M. T.; Deyab, M. A. Three new gemini ionic liquids: Synthesis, characterizations and anticorrosion applications. *J. Mol. Liq.* **2018**, *266*, 703−710.
(16) Chugh, B.; Singh, A. K.; Poddar, D.; Thakur, S.; Pani, B.; Jain, P. Relation of degree of substitution and metal protecting ability of cinnamaldehyde modified chitosan. *Carbohydr. Polym.* **2020**, *234*, No. 115945.
(17) Ashassi-Sorkhabi, H.; Shabani, B.; Aligholipour, B.; Seifzadeh, D. The effect of some Schiff bases on the corrosion of aluminum in hydrochloric acid solution. *Appl. Surf. Sci.* **2006**, *252* (12), 4039−4047.
(18) Ashmawy, A. M.; Attia, S. K.; Nessim, M. I.; Elnaggar, E. S. M.; El-Bassoussi, A. A. Study on some azo liquid crystals as antioxidants for local base oil. *Mol. Cryst. Liq. Cryst.* **2018**, *668* (1), 78−90.
(19) Ashmawy, A. M.; El-Sawy, A. M.; Ali, A. A.; El-Bahy, S. M.; Sayed Alahl, A. A., Oxidative stability performance of new azophenol derivatives as antioxidants in working fluids for high-temperature solar applications. *Sol. Energy Mater. Sol. Cells* **2021**, *230*. DOI: 10.1016/j.solmat.2021.111282.
(20) Ashmawy, A. M.; Nessim, M. I.; El-Dougdoug, W. I.; Attia, S. K.; Arief, M. H.; Zidane, M. H. Improving Oxidation Stability of Base Oil Based on Azophenols Additives: Experimental and Theoretical Studies. *Pet. Chem.* **2021**, *61* (11), 1275−1287.
(21) Abdulridha, A. A.; Albo Hay Allah, M. A.; Makki, S. Q.; Sert, Y.; Salman, H. E.; Balakit, A. A. Corrosion inhibition of carbon steel in 1 M H2SO4 using new Azo Schiff compound: Electrochemical, gravimetric, adsorption, surface and DFT studies. *J. Mol. Liq.* **2020**, *315*, No. 113690.
(22) Subasree, N.; Arockia Selvi, J.; Pillai, R. S. Effect of alkyl chain length on the corrosion inhibition of mild steel in a simulated hydrochloric acid medium by a phosphonium based inhibitor. *J. Adhes. Sci. Technol.* **2023**, *37*, 83−104.
(23) Guo, L.; Wu, M.; Kaya, S.; Chen, M.; Madkour, L. H. *In Influence of the alkyl chain length of alkyltriazoles on the Corrosion Inhibition of Iron: A DFTB Study*, AIP Conference Proceedings; AIP Publishing LLCPublishing LLC: 2018; 020015.
(24) Zhang, C.; Hu, J.; Yang, Z.; Zheng, Z.; Geng, S.; Zhong, X. Effects of the number of imidazoline ring and the length of alkyl group chain of imidazoline derivatives on corrosion inhibition of carbon steel in HCl solution: molecular simulation and experimental validation. *Petroleum* **2021**, *8*, 447−457.
(25) Deyab, M. A.; Fouda, A. S.; Osman, M. M.; Abdel-Fattah, S. Mitigation of acid corrosion on carbon steel by novel pyrazolone derivatives. *RSC Adv.* **2017**, *7*, 45232−45240.
(26) Shokry, H.; El-Wekeal, N.; Issa, R. Influence of Some Azo—Azomethine Compounds and Their Complexes on the Corrosion Inhibition of Copper in Chloride Media. *Adsorp. Sci. Technol.* **2005**, *23* (8), 643−654.
(27) Nagiub, A. M.; Mahross, M.; Khalil, H.; Mahran, B.; Yehia, M.; El-Sabbah, M. Azo dye compounds as corrosion inhibitors for dissolution of mild steel in hydrochloric acid solution. *Port. Electrochim. Acta* **2013**, *31* (2), 119−139.
(28) Elaryian, H. M.; Bedair, M. A.; Bedair, A. H.; Aboushahba, R. M.; Fouda, A. E.-A. S. Synthesis, characterization of novel coumarin dyes as corrosion inhibitors for mild steel in acidic environment: Experimental, theoretical, and biological studies. *J. Mol. Liq.* **2022**, *346*, No. 118310.
(29) Ashmawy, A. M.; Nessim, M. I.; Elnaggar, E. M.; Osman, D. I. Preparation and evaluation of some novel liquid crystals as antioxidants. *Mol. Cryst. Liq. Cryst.* **2017**, *643* (1), 188−198.
(30) Deyab, M. A.; Mele, G. Stainless steel bipolar plate coated with polyaniline/Zn-Porphyrin composites coatings for proton exchange membrane fuel cell. *Sci. Rep.* **2020**, *10*, No. 3277.
(31) Deghadi, R. G.; Elsharkawy, A. E.; Ashmawy, A. M.; Mohamed, G. G. Antibacterial and anticorrosion behavior of bioactive complexes

of selected transition metal ions with new 2-acetylpyridine Schiff base. *Appl. Organomet. Chem.* **2022**, *36* (4), No. e6579.
(32) Mohammed, H. A.; Mostafa, H. Y.; El-Aty, D. M. A.; Ashmawy, A. M. Novel Gemini ionic liquid for oxidative desulfurization of gas oil. *Sci. Rep.* **2023**, *13* (1), No. 6198.
(33) Deyab, M. A.; Guibal, E. Enhancement of corrosion resistance of the cooling systems in desalination plants by green inhibitor. *Sci. Rep* **2020**, *10*, 4812.
(34) Deyab, M. A. Understanding the anti-corrosion mechanism and performance of ionic liquids in desalination, petroleum, pickling, descaling, and acid cleaning applications. *J. Mol. Liq.* **2020**, *309*, No. 113107.
(35) Mostafa, M. A.; Ashmawy, A. M.; Reheim, M. A. M. A.; Bedair, M. A.; Abuelela, A. M. Molecular structure aspects and molecular reactivity of some triazole derivatives for corrosion inhibition of aluminum in 1 M HCl solution. *J. Mol. Struct.* **2021**, *1236*, No. 130292.
(36) Deyab, M. A.; Mele, G.; Al-Sabagh, A. M.; Bloise, E.; Lomonaco, D.; Mazzetto, S. E.; Clemente, C. D. S. Synthesis and characteristics of alkyd resin/M-Porphyrins nanocomposite for corrosion protection application. *Prog. Org. Coat.* **2017**, *105*, 286−290.
(37) Yadav, M.; Kumar, S.; Bahadur, I.; Ramjugernath, D. Corrosion inhibitive effect of synthesized thiourea derivatives on mild steel in a 15% HCl solution. *Int. J. Electrochem. Sci.* **2014**, *9* (11), 6529−6550.
(38) Deyab, M. A.; Mele, G. Polyaniline/Zn-phthalocyanines nanocomposite for protecting zinc electrode in Zn-air battery. *J. Power Sources* **2019**, *443*, No. 227264.
(39) Deyab, M. A.; Abd El-Rehim, S. S. On surfactant-polymer association and its effect on the corrosion behaviour of carbon steel in cyclohexane propionic acid. *Corros. Sci.* **2012**, *65*, 309−316.
(40) Deyab, M. A.; El-Shamy, O. A. A.; Thabet, H. K.; Ashmawy, A. M. Electrochemical and theoretical investigations of favipiravir drug performance as ecologically benign corrosion inhibitor for aluminum alloy in acid solution. *Sci. Rep.* **2023**, *13* (1), No. 8680.

https://doi.org/10.1021/acsomega.3c06710
ACS Omega 2023, 8, 49009−49016